Out-of-Plane Shake-Table Tests on Unreinforced Masonry Gables Considering Different Roof Configurations

Nicolò Damiani[1,2(✉)], Marta Bertassi[3], Satyadhrik Sharma[4], Marco Smerilli[2], Michele Mirra[4], Igor Lanese[2], Elisa Rizzo-Parisi[2], Gerard J. O'Reilly[2,3], Francesco Messali[4], and Francesco Graziotti[1,2]

[1] Department of Civil Engineering and Architecture (DICAr), University of Pavia, Pavia, Italy
nicolo.damiani@unipv.it
[2] European Centre for Training and Research in Earthquake Engineering (EUCENTRE), Pavia, Italy
[3] University School for Advanced Studies IUSS Pavia, Pavia, Italy
[4] Faculty of Civil Engineering and Geosciences, University of Technology of Delft (TU Delft), Delft, The Netherlands

Abstract. Low-rise masonry buildings worldwide frequently feature unreinforced masonry (URM) walls coupled with various pitched roof configurations supported by masonry gables. Past earthquakes have highlighted the vulnerability of these components to out-of-plane seismic loads due to their high slenderness, insufficient roof connections, and exposure to amplified accelerations while being subjected to minimal overburden due to their location at the upper part of buildings. This study presents key insights from the experimental campaign of the ERIES-SUPREME project, aimed at enhancing the understanding of the out-of-plane seismic behavior of masonry gables. Incremental dynamic tests were performed on three full-scale URM gables, simulating both induced and tectonic earthquake scenarios until collapse, using two shake tables. Differential motions at the top and bottom tables reproduced the interaction of the gables with three different roof diaphragm configurations, each introducing a unique filtering effect on the seismic input. The outcomes of the experiments can be used for refining existing numerical modelling strategies as well as contribute to developing improved tools for the seismic assessment of URM gables.

Keywords: Differential input motions · Gable walls · Incremental dynamic shake-table tests · Roof stiffness · Out of plane · Unreinforced Masonry

1 Introduction

Unreinforced masonry (URM) structures form a significant portion of the building stock in many areas worldwide. These structures often exhibit a relevant seismic vulnerability, mainly attributable to the poor material mechanical properties, and to the lack

G. O'Reilly and G. M. Calvi (Eds.): ERIES-IW 2025, LNCE 718, pp. 268–279, 2025.
https://doi.org/10.1007/978-3-031-98893-6_25

of adequate detailing to prevent local failures such as wall out-of-plane (OOP) overturning. This vulnerability has been documented in post-earthquake damage surveys reported in numerous studies [1–4]. These structures are prevalent in seismically active regions, including areas affected by both natural and induced seismicity. Typical low-rise masonry buildings consist of URM walls with different timber roof configurations, generally supported by masonry gables. Post-earthquake damage surveys and experimental evidence [5, 6] recognized masonry gables as structural elements significantly vulnerable to OOP failures. Their vulnerability is mostly attributed to their high slenderness, weak connections to the roof structure, and location at the top of the building where seismic amplification is typically most pronounced. This location exposes them to amplified seismic excitation compared to the motion at the ground, while they are subjected to minimal vertical overburden loads. Nonetheless, experimental and numerical investigations on the seismic response of URM gable walls remain limited in the literature [7, 8], with most studies focusing on walls with rectangular geometries [9–15], leaving a gap in the understanding of the gable behavior under seismic loading.

To address this gap, this paper presents a dynamic full-scale shake-table testing campaign on three full-scale URM gables to investigate their seismic behavior until complete collapse. The tested gable specimens and their material properties are first described. Although the roof was not explicitly included in the experiments, the effect of its stiffness on the gable response is accounted for by applying differential input motions through two shake tables: one at the gable base and another at its top. A detailed description of the experimental setup is then provided. Input motions representative of both induced and tectonic seismicity were applied to the shake tables and are described alongside the incremental dynamic testing sequence. Finally, the main experimental results are presented, comparing the response of the three gables interacting with roofs of varying stiffness. All experimental data, and the associated instrumentation schemes, are openly available for download at https://doi.org/https://doi.org/10.60756/euc-1avy7q49 [16].

2 Description and Mechanical Characterization of the Masonry Specimens

2.1 Specimen Geometry

The test specimens of the experimental campaign consisted of three identical full-scale URM gable walls, which were built on a composite steel-concrete foundation. Each specimen had a length of 6 m and height of 3 m. The gables were built using clay bricks, with average dimensions of 230 × 105 × 55 mm, resulting in a gable thickness of 105 mm. The gables consisted of 45 courses of bricks, and all mortar joints were 10-mm-thick (Fig. 1).

Moreover, five joist pockets were realized to accommodate the timber beams of the roof, with a cross-section of 100 × 200 mm. These beams were used to transfer the vertical load representative of the roof diaphragm weight, resulting in an overburden of 0.07 MPa at the mid-height of the gable. Hence, a vertical load of 4.5 kN was applied through each timber beam, resulting in a total vertical load of 22.5 kN, simulating half

the weight of a typical timber roof diaphragm, consistent with the geometry of the tested gable specimen. These beams were also used to apply lateral loads along the height of the specimen, as further discussed in the following sections.

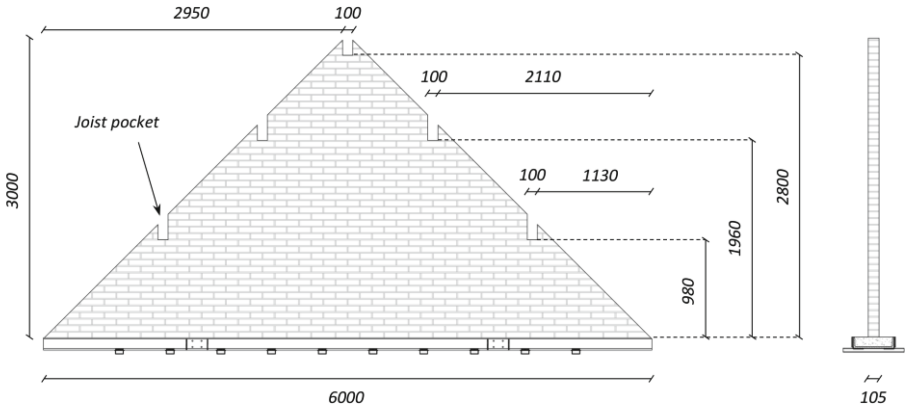

Fig. 1. Full-scale masonry gable specimen details and pictures. Units of mm.

The experimental tests were conducted without steel anchors between the timber joists and masonry gables. This approach simulated a "worst-case" scenario, where timber-to-masonry connections relied entirely on friction, providing a lower-bound estimate of the gable seismic resistance.

2.2 Summary of Material Mechanical Properties

The tested gable specimens were accompanied by complementary material characterization performed on unit, mortar, and masonry as a composite material. All material characterization tests were performed at the "Giorgio Macchi" Material and Structural Testing Laboratory of the Department of Civil Engineering and Architecture (DICAr) of the University of Pavia (Italy), on specimens that reached 28 days of maturation.

The characterization included the compressive (f_c) and flexural strength (f_t) of mortar, the compressive (f_u) strength of bricks, the compressive strength (f_m) of masonry perpendicular to bed joints, and secant elastic modulus (E_m) calculated between 10 and 33% of f_m, the bond strength (f_w) of masonry, the initial shear strength (f_{v0}) and friction coefficient (μ). All tests were performed following the latest applicable European norms [17–21]. Furthermore, to characterize the response of masonry bed joints under torsional shear stress ($f_{v0,tor}$, μ_{tor} evaluated assuming a linear elastic hypothesis), a dedicated test was performed [22]. The density of masonry (ρ_m) was determined from the average weight of the tested gables. Table 1 summarizes experimental mean values and coefficient of variation (C.o.V.) for the investigated mechanical properties.

Table 1. Summary of unit, mortar and masonry mechanical properties.

Material properties	Symbol	Units	Mean	C.o.V
Mortar compressive strength	f_c	[MPa]	0.68	0.26
Mortar flexural strength	f_t	[MPa]	0.20	0.50
Unit/brick compressive strength	f_u	[MPa]	42.57	0.09
Masonry compressive strength	f_m	[MPa]	7.44	0.10
Masonry elastic modulus	E_m	[MPa]	4072	0.11
Masonry initial shear strength	f_{v0}	[MPa]	0.19	–
Masonry friction coefficient	μ	[-]	0.51	–
Masonry bond strength	f_w	[MPa]	0.21	0.48
Masonry initial shear strength (torsional)	$f_{v0,tor}$	[MPa]	0.42	–
Masonry friction coefficient (torsional)	μ_{tor}	[-]	1.15	–
Masonry density	ρ_m	[kg/m^3]	1883	–

3 Testing Layout and Setup

3.1 Testing Layout

Three dynamic shake-table tests on full-scale masonry gables were performed at the 9D LAB of the EUCENTRE facilities in Pavia, Italy. This advanced seismic testing system features a dual shake-table configuration, including a top and bottom table capable of applying differential input motions covering nine degrees of freedom. This setup enables reproducing interstorey displacements occurring during earthquakes. The 9D LAB, with its 4.8 $\times$ 4.8 m dimensions, was large enough to accommodate the full-scale gable walls but not an entire roof diaphragm. To account for the influence of roof stiffness on the OOP seismic response of the gables, variations in the input motion imposed on the top shake table were introduced. In particular, three different configurations for the roof structure were considered: (i) Gable1-STIFF, representing a stiff roof diaphragm, where the top shake table replicated the motion of the bottom table; (ii) Gable2-SEMIFLEX, representing an intermediate case, where the top motion was linearly amplified relative to the base motion; and (iii) Gable3-FLEX, simulating a flexible roof diaphragm, where the motion at the top was significantly amplified and phase-shifted relative to the base motion.

3.2 Testing Setup

The experimental setup, depicted in Fig. 2, consisted of a dual shake-table configuration, including a top and bottom table capable of applying differential input motions. The test setup included a loading frame, composed of shaped profiles, that transferred accelerations along the gable height through five horizontal loading arms hinged to the frame. Timber beams were screwed to the steel arms to replicate the presence of timber joists typically found in real roof structures. The five horizontal loading arms also

allowed applying the vertical loads to the gable specimens through five springs, one for each loading arm. These loads were applied to the gable specimens by pulling down the horizontal steel arms through steel bars in series with the springs (Fig. 3).

It is worth to note that the loading frame was hinged at both the bottom and top shake tables to avoid introducing additional OOP stiffness and strength to the gable specimen, whose foundation was fixed to the bottom shake table. A stiff instrumentation frame, anchored to the bottom shake table, completed the test setup serving as support and a fixed reference for the instruments.

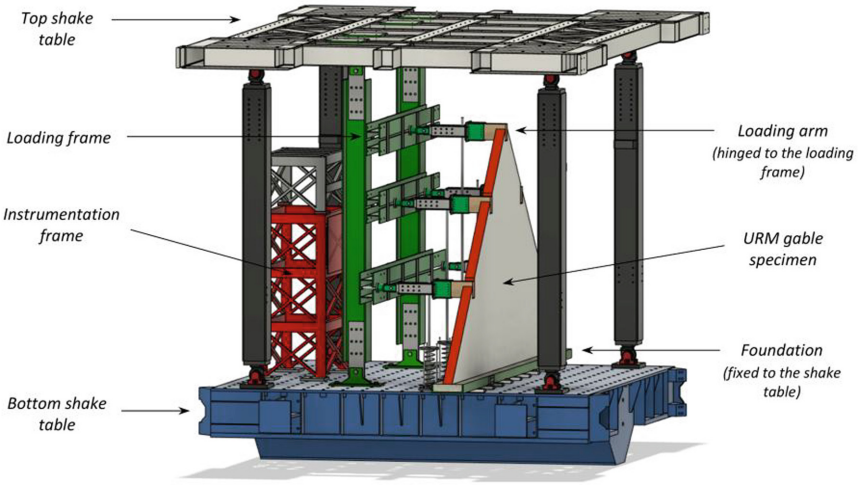

Fig. 2. Three-dimensional view of the shake-table testing setup of the 9D LAB.

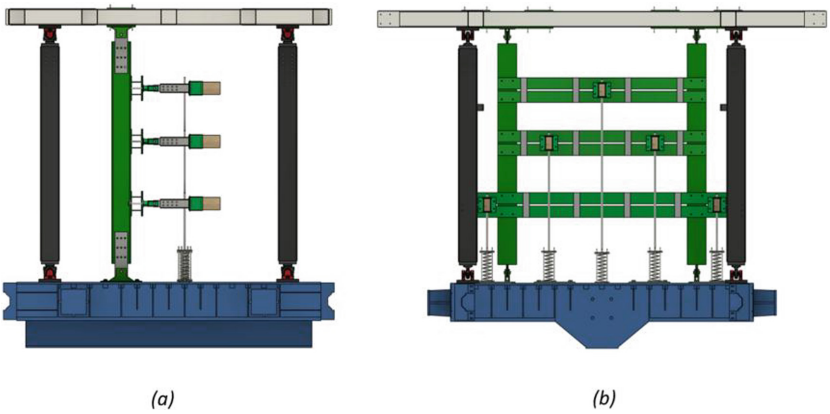

Fig. 3. Lateral (a) and front (b) views of the installed loading frame.

A key feature of this experimental setup is its ability to precisely control the boundary conditions of each masonry gable, ensuring that its seismic response remains independent

of the loading frame. As illustrated in Fig. 4, during the shake-table test, the gable specimen is expected to rotate by pivoting at its base, altering the support conditions of the timber beams. Consequently, rather than being evenly distributed across the full gable thickness, the vertical load applied through the pre-compressed springs results concentrated at a single point. However, since this load remains perpendicular to the bottom shake table, it has minimal impact on the gable specimen out-of-plane seismic response.

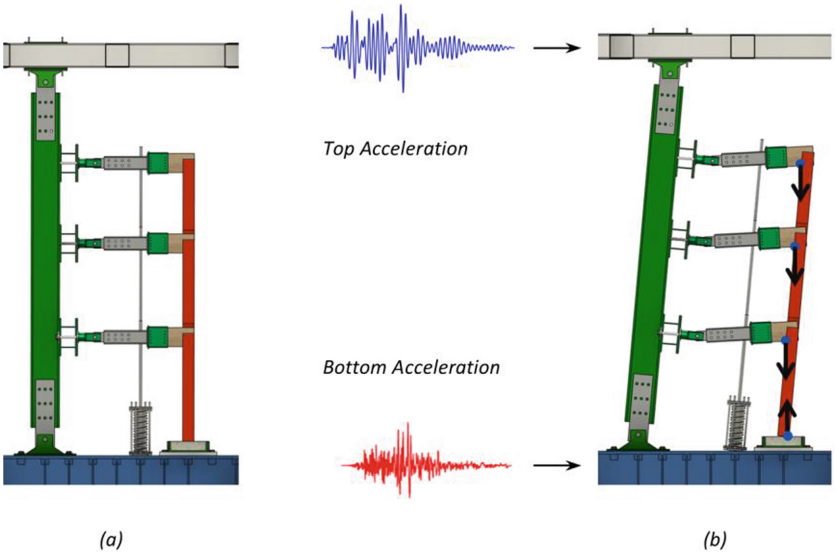

Fig. 4. Representation of the vertical load application during the test: (a) undeformed configuration of the specimen and loading frame; (b) deformed configuration of the specimen and loading frame under differential seismic input.

4 Instrumentation, Input Signals, and Testing Protocols

4.1 Instrumentation and Data Acquisition

The instrumentation installed on each gable included accelerometers, potentiometers, wire potentiometers, and a 3D optical acquisition system. The positioning of the instruments was determined based on the expected deformed shapes and cracking patterns. Accelerometers were installed on the gable specimens to record acceleration-time histories, with additional units placed on the loading and instrumentation frames, as well as on the specimen foundation. Potentiometers were used to measure the elongation or shortening of springs and the relative displacements between the timber beams and the masonry. Wire potentiometers, attached to both the loading and instrumentation frames, were used to record displacements of the gable specimens. Finally, the optical monitoring system was employed to measure displacements on the free surface of the gable, opposite to the loading frame.

4.2 Input Signals

The 9D LAB setup enabled the application of distinct input motions at the bottom and top shake tables, simulating the influence of roof diaphragm in-plane stiffness. Two alternative floor motion (FM) scenarios were considered: FM1, representing induced seismicity, and FM2, associated with tectonic seismicity. For the induced scenario, numerical analyses were performed on a finite element model of a typical URM building from the Groningen region in the Netherlands. The building was assessed in its as-built conditions with a flexible timber roof, and in two alternative retrofitted configurations: one with a rigid concrete roof and another incorporating a timber-based retrofit intervention resulting in a semi-flexible roof. In the tectonic seismicity scenario, recorded data from the 2016 Central Italy earthquake, collected at the attic level of a monitored masonry building, were utilized. In this case, the interaction between the gable and the roof was modeled using an elastic single-degree-of-freedom system. Further details on input signal selection can be found in [23].

Figure 5 presents the induced and tectonic input signals at the bottom (i.e., attic floor) and top (i.e., ridge beam) levels of the gable, along with the corresponding elastic response spectra for a 5% viscous damping ratio.

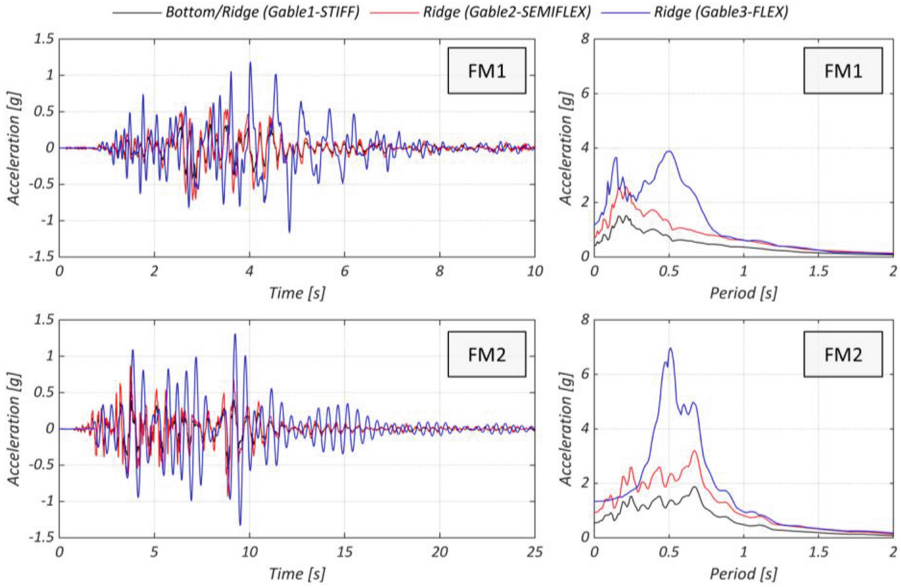

Fig. 5. Summary of acceleration time histories (left) and elastic response spectra (right).

4.3 Testing Protocols

The incremental dynamic test (IDT) for each gable specimen was conducted using both input signals: first the induced (FM1), followed by the tectonic (FM2), with a scaling factor (SF) linearly adjusted based on the bottom input signal. The parameters presented in Table 2, Table 3, and Table 4 include *PBA* (peak base acceleration), *PRA*

(peak ridge acceleration) and Δ_d (ridge beam displacement relative to the bottom shake table). Each of these values is reported both as the nominal (i.e., target theoretical) value corresponding to the input signals in Fig. 5 and as the experimentally recorded value. Moreover, the maximum displacement of a control point on the gable, max(d_{ctrl}), is included. The location of the control point varied with the progression of damage. During the initial tests, before the collapse mechanism was activated, the control point was set at the barycenter of the gable. In later tests, as collapse mechanisms developed, it was relocated to the horizontal crack responsible for failure, which was specific to each gable. When this point was not directly instrumented, its location was determined through trigonometric calculations. Furthermore, all displacement calculations exclude any rigid displacement of the loading frame.

For Gable1-STIFF (Table 2), the nominal Δ_d was zero. However, this condition could not be replicated experimentally due to the difficulty in achieving perfectly simultaneous movement of the bottom and top shake tables. To proceed with the IDT, the tectonic record was scaled up to gable collapse to explore not only higher earthquake motion intensities but also signals with different frequencies and longer durations. It should be noted that for Gable3-FLEX, an additional shake-table test at 100% FM1 was conducted after Test #9 (i.e., the 100% FM2 run) to evaluate its ability to withstand an induced seismic motion after sustaining damage from tectonic motion.

Table 2. Testing sequence of Gable1-STIFF.

Test #		SF	Nom. *PBA* [g]	Rec. *PBA* [g]	Nom. *PRA* [g]	Rec *PRA* [g]	Nom. Δ_d [mm]	Rec Δ_d [mm]	max(d_{ctrl}) [mm]
1	FM1	10%	0.04	0.05	0.04	0.13	0	1.7	0.2
2		20%	0.08	0.08	0.08	0.19	0	1.6	0.4
3		30%	0.13	0.12	0.13	0.26	0	2.6	0.4
4		50%	0.21	0.19	0.21	0.39	0	4.6	0.5
5		75%	0.32	0.28	0.32	0.49	0	7.1	0.6
6		100%	0.42	0.37	0.42	0.61	0	8.9	0.7
7	FM2	50%	0.27	0.29	0.27	0.44	0	7.2	0.7
8		75%	0.41	0.43	0.41	0.53	0	10.5	0.8
9		100%	0.55	0.57	0.55	0.71	0	13.0	1.0
10		125%	0.69	0.69	0.69	0.84	0	16.4	1.3
11		150%	0.82	0.86	0.82	0.96	0	19.3	1.5
12		175%	0.96	1.03	0.96	1.19	0	23.3	1.9
13		200%	1.10	1.17	1.10	1.34	0	25.5	2.1
14		250%	1.38	1.51	1.38	1.64	0	31.8	5.5
15		300%	1.65	1.88	1.65	1.86	0	38.1	48.9
16		350%	1.93	1.80	1.93	2.56	0	34.8	collapse

Table 3. Testing sequence of Gable2-SEMIFLEX.

Test #		SF	Nom. *PBA* [g]	Rec. *PBA* [g]	Nom. *PRA* [g]	Rec *PRA* [g]	Nom. Δ_d [mm]	Rec Δ_d [mm]	max(d_{ctrl}) [mm]
1	FM1	10%	0.04	0.05	0.08	0.16	2.5	2.0	0.03
2		20%	0.08	0.08	0.16	0.29	5.1	4.4	0.1
3		30%	0.13	0.12	0.23	0.36	7.6	6.7	0.2
4		50%	0.21	0.20	0.39	0.45	12.7	10.6	0.3
5		75%	0.32	0.28	0.58	0.62	19.0	15.3	0.5
6		100%	0.42	0.38	0.78	0.81	25.3	19.9	0.7
7	FM2	50%	0.27	0.28	0.43	0.62	21.3	16.6	0.5
8		75%	0.41	0.42	0.64	0.93	31.9	24.1	0.8
9		100%	0.55	0.57	0.85	1.26	42.5	41.1	2.8
10		125%	0.69	0.71	1.06	1.46	53.2	50.5	4.9
11		150%	0.82	0.86	1.28	1.86	63.8	59.9	8.7
12		175%	0.96	1.00	1.49	2.15	74.4	71.2	29.9
13		200%	1.10	1.04	1.70	3.31	85.1	88.5	88.6

Table 4. Testing sequence of Gable3-FLEX.

Test #		SF	Nom. *PBA* [g]	Rec. *PBA* [g]	Nom. *PRA* [g]	Rec *PRA* [g]	Nom. Δ_d [mm]	Rec Δ_d [mm]	max(d_{ctrl}) [mm]
1	FM1	10%	0.04	0.05	0.12	0.31	5.7	5.9	0.3
2		20%	0.08	0.09	0.24	0.53	11.4	12.1	0.6
3		30%	0.13	0.13	0.36	0.55	17.0	16.0	0.8
4		50%	0.21	0.20	0.60	0.84	28.4	26.7	1.2
5		75%	0.32	0.28	0.90	1.10	42.6	39.8	2.3
6		100%	0.42	0.36	1.20	1.33	56.8	52.8	3.2
7	FM2	50%	0.27	0.28	0.65	0.79	41.1	40.4	2.4
8		75%	0.41	0.43	0.97	1.28	61.6	57.0	3.8
9		100%	0.55	0.57	1.30	1.91	82.2	85.9	30.2
10		125%	0.42	0.36	1.20	1.33	56.8	53.9	18.5
11		150%	0.69	0.70	1.62	2.34	102.7	107.5	33.4
12		175%	0.82	0.85	1.95	2.56	123.3	112.2	collapse

5 Incremental Dynamic Response

The main outcomes of the full-scale shake-table experiments are presented in Fig. 6 in terms of seismic capacity curves, for each gable specimen (Gable1-STIFF, Gable2-SEMIFLEX, Gable3-FLEX). These curves depict the maximum displacement of the control point (max(d_{ctrl})) versus the peak base acceleration (*PBA*), at each input scaling level.

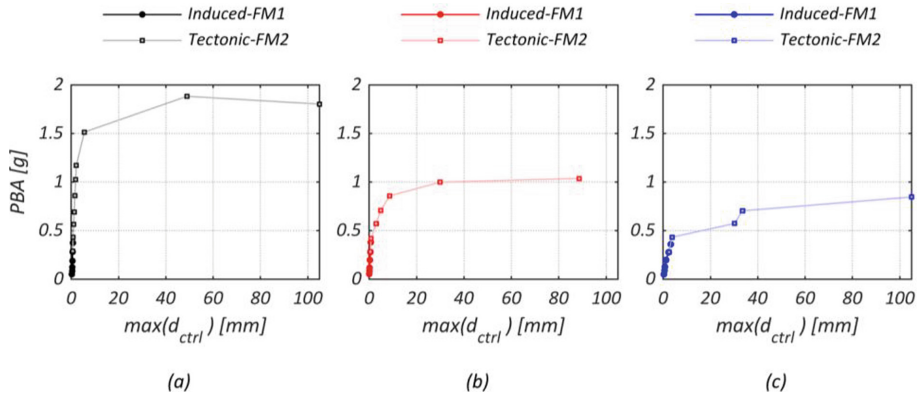

Fig. 6. Capacity curves for: (a) Gable1-STIFF, (b) Gable2-SEMIFLEX, and (c) Gable3-FLEX.

Gable1-STIFF (Fig. 6a) exhibited an initial elastic behavior from Test #1 through Test #13, while a notable change in stiffness occurred in Test #14. Gable 2-SEMIFLEX (Fig. 6b) remained seemingly elastic until Test #9, while collapse occurred at Test #13, corresponding to a scale factor of 200%. Finally, Gable 3-FLEX displayed elastic behavior until Test #8, but by Test #9, a shift in slope became apparent.

The influence of roof flexibility on the seismic response of URM gables is evident when comparing all three capacity curves. Gable3-FLEX demonstrated significantly lower seismic capacity and substantially greater flexibility, indicating higher vulnerability compared to the other configurations.

6 Conclusions

This paper presented an extensive experimental investigation into the out-of-plane (OOP) seismic behavior of unreinforced masonry (URM) gables through a full-scale shake-table testing campaign. The research was conducted at the EUCENTRE 9D LAB (Pavia, Italy), using an innovative dual shake-table configuration that simulated the interaction between URM gables and different roof diaphragm configurations. The primary aim behind this was to evaluate the seismic response of these structural elements and understand the influence of varying roof stiffness levels on their failure mechanisms.

The results, in terms of incremental dynamic response, demonstrate that roof diaphragm stiffness plays a key role in governing the seismic performance of URM

gables. The experimental results indicate that Gable1-STIFF, representing a stiff roof diaphragm, exhibited the highest resistance to OOP loading, minimizing differential displacements. Gable2-SEMIFLEX, simulating a semi-flexible roof, showed intermediate behavior, with lower resistance and earlier crack formation compared to the stiff configuration. Gable3-FLEX, representing a flexible roof diaphragm, had the lowest acceleration capacity, emphasizing the effects of reduced roof stiffness on gable wall stability. These findings confirm that flexible roof diaphragms amplify OOP displacements and increase masonry gable vulnerability.

This research advances seismic risk mitigation strategies for low-rise masonry structures. The insights gained provide a benchmark for improving code-based guidelines, building design, and retrofitting strategies in earthquake-prone regions worldwide.

Acknowledgements. This work is part of the transnational access project "ERIES-SUPREME", supported by the Engineering Research Infrastructures for European Synergies (ERIES) project (www.eries.eu), which has received funding from the European Union's Horizon Europe Framework Programme under Grant Agreement No. 101058684. This is ERIES publication number C64. Additional funds required beyond the scope of the ERIES grant for the realisation of the project were provided by the partner "TNO: Netherlands Organisation for Applied Scientific Research/Nederlandse Organisatie voor Toegepast Natuurwetenschappelijk Onderzoek".

References

1. Ingham, J., Griffith, M.: Performance of unreinforced masonry buildings during the 2010 Darfield (Christchurch, NZ) earthquake. Aust. J. Struct. Eng. **11**(3), 207–224 (2010)
2. Dizhur, D., et al.: Performance of masonry buildings and churches in the 22 February 2011 Christchurch earthquake. Bull. N. Z. Soc. Earthq. Eng. **44**(4), 279–296 (2011)
3. Penna, A., Morandi, P., Rota, M., Manzini, C.F., Da Porto, F., Magenes, G.: Performance of masonry buildings during the Emilia 2012 earthquake. Bull. Earthq. Eng. **12**, 2255–2273 (2014)
4. Sorrentino, L., Liberatore, L., Liberatore, D., Masiani, R.: The behaviour of vernacular buildings in the 2012 Emilia earthquakes. Bull. Earthq. Eng. **12**, 2367–2382 (2014)
5. Graziotti, F., Tomassetti, U., Kallioras, S., Penna, A., Magenes, G.: Shaking table test on a full scale URM cavity wall building. Bull. Earthq. Eng. **15**, 5329–5364 (2017)
6. Kallioras, S., Correia, A.A., Graziotti, F., Penna, A., Magenes, G.: Collapse shake-table testing of a clay URM building with chimneys. Bull. Earthq. Eng. **18**(3), 1009–1048 (2019)
7. Candeias, P.X., Costa, A.C., Mendes, N., Costa, A.A., Lourenço, P.B.: Experimental assessment of the out-of-plane performance of masonry buildings through shaking table tests. Int. J. Archit. Herit. **11**(31), 31–58 (2016)
8. Tomassetti, U., Correia, A.A., Graziotti, F., Penna, A.: Seismic vulnerability of roof systems combining URM gable walls and timber diaphragms. Earthquake Eng. Struct. Dynam. **48**, 1297–1318 (2019)
9. Griffith, M.C., Lam, N.T.K., Wilson, J.L., Doherty, K.: Experimental investigation of unreinforced brick masonry walls in flexure. J. Struct. Eng. **130**(3), 423–432 (2004)
10. Penner, O., Elwood, K.J.: Out-of-plane dynamic stability of unreinforced masonry walls in one-way bending: Parametric study and assessment guidelines. Earthq. Spectra **32**, 1699–1723 (2016)
11. Giaretton, M., Dizhur, D., Ingham, J.M.: Dynamic testing of as-built clay brick unreinforced masonry parapets. Eng. Struct. **127**, 676–685 (2016)

12. Graziotti, F., Tomassetti, U., Penna, A., Magenes, G.: Out-of-plane shaking table tests on URM single leaf and cavity walls. Eng. Struct. **125**, 455–470 (2016)
13. Sharma, S., Tomassetti, U., Grottoli, L., Graziotti, F.: Two-way bending experimental response of URM walls subjected to combined horizontal and vertical seismic excitation. Eng. Struct. **219**, 110537 (2020)
14. Tomassetti, U., Grottoli, L., Sharma, S., Graziotti, F.: Dataset from dynamic shake-table testing of five full-scale single leaf and cavity URM walls subjected to out-of-plane two-way bending. Data Brief **24**, 103854 (2019)
15. Sharma, S., Grottoli, L., Tomassetti, U., Graziotti, F.: Dataset from shake-table testing of four full-scale URM walls in a two-way bending configuration subjected to combined out-of-plane horizontal and vertical excitation. Data Brief **31**, 105851 (2020)
16. Sharma, S., et al.: Experimental data from out-of-plane shake-table tests on unreinforced masonry gables. Earthq. Spectra (2025)
17. European Committee for Standardization (CEN): Methods of test for mortar for masonry. Part 11: Determination of flexural and compressive strength of hardened mortar. European Standard EN 1015-11, Brussels, Belgium (2006)
18. European Committee for Standardization (CEN): Methods of test for masonry units. Part 1: Determination of compressive strength. European Standard EN 772-1, Brussels, Belgium (2006)
19. European Committee for Standardization (CEN): Methods of test for masonry. Part 1: Determination of compressive strength. European Standard EN 1052-1, Brussels, Belgium (1998)
20. European Committee for Standardization (CEN): Methods of test for masonry. Part 5: Determination of bond strength by the Bond Wrench method. European Standard EN 1052-5, Brussels, Belgium (2005)
21. European Committee for Standardization (CEN): Methods of test for masonry units. Part 3: Determination of initial shear strength. European Standard EN 1052-3, Brussels, Belgium (2007)
22. Sharma, S., Graziotti, F., Magenes, G.: Torsional shear strength of unreinforced brick masonry bed joints. Constr. Build. Mater. **275**, 122053 (2021)
23. Mirra, M., Damiani, N., Sharma, S., Graziotti, F., Messali, F.: Definition of differential seismic input motions for out-of-plane dynamic testing of unreinforced masonry gable walls considering different roof configurations. Structures **79**, 109419 (2025). https://doi.org/10.1016/j.istruc.2025.109419